ADVANCED FUNCTIONAL MATERIALS
www.afm-journal.de

Blood-Inert Surfaces via Ion-Pair Anchoring of Zwitterionic Copolymer Brushes in Human Whole Blood

Yung Chang, Yu-Ju Shih, Chia-Jung Lai, Hsiao-Han Kung, and Shaoyi Jiang**

A strategy to create blood-inert surfaces in human whole blood via ion-pair anchoring of zwitterionic copolymer brushesand a systematic study of how well-defined chain lengths and well-controlled surface packing densities of zwitterionic polymers affect blood compatibility are reported. Well-defined diblock copolymers, poly(11-mercaptoundecyl sulfonic acid)-*block*-poly-(sulfobetaine methacrylate) (PSA-*b*-PSBMA) with varying zwitterionic PSBMA or negatively charged PSA lengths, are synthesized via atom-transfer radical polymerization (ATRP). PSA-*b*-PSBMA is grafted onto a surface covered with polycation brushes as a mimic polar/hydrophilic biomaterial surface via ion-pair anchoring at a range of copolymer concentrations. Protein adsorption from single-protein solutions, 100% blood serum, and 100% blood plasma onto the surfaces covered with PSA-*b*-PSBMA brushes is evaluated using a surface plasmon resonance sensor. Copolymer brushes containing a high amount of zwitterionic SBMA units are further challenged with human whole blood. Low protein-fouling surfaces with >90% reduction with respect to uncoated surfaces are achieved with longer PSA blocks and higher concentrations of PSA-*b*-PSBMA copolymers using the ion-pair anchoring approach. This work provides a platform to achieve the control of various surface parameters and a practical method to create blood-inert surfaces in whole blood by grafting ionic-zwitterionic copolymers to charged biomaterials via charge pairing.

1. Introduction

A fundamental understanding of blood-inert surfaces resisting the adsorption of plasma proteins and the adhesion of blood cells is highly desirable and critically important in the development of blood-contacting biomaterials in such applications as blood collection devices, antithrombogenic implants, hemodialysis membranes, drug-delivery carriers, and diagnostic biosensors.[1–3] The interactions of clotting factors, plasma proteins and platelets on blood-contacting materials strongly affect the thrombotic reaction induced by intrinsic surface contact.[4,5] To minimize the thrombogenicity of biomaterials, heparinized materials are often used to prolong blood clotting time when they are coated on the surfaces of blood-contacting devices or containers.[6–8] Nonspecific adsorption of proteins such as fibrinogen and clotting enzymes is recognized as the first interaction event to induce a full-scale platelet adhesion and activation, leading to thrombosis and embolism at the blood-material interface.[9] Hence, protein-resistant surfaces have been widely investigated in order to achieve no blood clot formation.[10–12] It is now recognized that the retention of bound water molecules surrounding the functional groups of material interfaces plays a key role in surface resistance to nonspecific protein adsorption.[13–15] Thus, to suppress nonspecific protein adsorption onto biomaterials, many studies have been carried out on surfaces grafted with poly(ethylene glycol) (PEG).[16–18] PEGylated surfaces face the problem of chemical stability in the presence of oxygen and transition-metal ions found in most biochemical solutions.[19,20] It was also shown that grafted PEG brushes lose their protein repulsive properties at physiological temperature.[21] In this regard, it is of great interest to have alternative nonfouling surfaces beyond PEG.

Zwitterionic biomaterials have received growing attention for use as blood-inert surfaces because of their excellent inhibition in plasma protein adsorption, blood platelet adhesion and activation, and thrombus formation in vitro.[22–24] A general characteristic of zwitterionic materials, including phosphobetaine, sulfobetaine or carboxylbetaine, is that they have both cationic and anionic charged moieties on the same side chain, maintaining overall charge neutrality.[25–30] As shown in previous work, zwitterionic betaines generate a tightly bound, structured water layer around the zwitterionic head groups via electrostatically induced hydration.[14–31] In recent years, zwitterionic poly(sulfobetaine methacrylate) (PSBMA) has been widely studied due to its ease of synthesis. It was reported that the blood-inert nature of zwitterionic PSBMA polymers is attributed to their strong hydration capabilities and conformational structures.[12,32–34]

Surface grafting is an effective approach to incorporate zwitterionic brushes onto a wide range of materials for improved blood compatibility. Two major strategies have been shown to prepare zwitterionic brushes, including grafting-from and

Prof. Y. Chang, Y.-J. Shih, C.-J. Lai, H.-H. Kung
R&D Center for Membrane Technology and
Department of Chemical Engineering
Chung Yuan Christian University
Chung-Li, Taoyuan 320, Taiwan
E-mail: ychang@cycu.edu.tw
Prof. S. Jiang
Department of Chemical Engineering
University of Washington
Seattle, WA 98195, USA
E-mail: sjiang@u.washington.edu

DOI: 10.1002/adfm.201201386

grafting-to.[28,29,35–41] Most of zwitterionic brushes produced by the grafting-from approach are prepared using surface-initiated controlled/living radical polymerization techniques, allowing accurate control over brush thickness, composition, and architecture to achieve high surface packing densities.[28,35–38] However, it is harder to implement nonfouling surface treatments in complex geometric shapes and large-scale processes. Thus, the grafting-to approach, involving the attachment of zwitterionic polymers via either chemisorption or physisorption, is a convenient route for preparing nonfouling biomaterials or coatings on a large scale or in complex geometries. However, unlike the grafting-from approach, the success of the graft-to approach depends on the ability to achieve high surface packing densities. There are several prior studies of low biofouling surface brushes via hydrophobic- or charge-driven assembled copolymers.[29,39,40] A recent study reported a successful grafting-to approach of physically adsorbed diblock copolymers containing zwitterionic PSBMA and hydrophobic moieties to achieve a superlow biofouling surface.[29] It was demonstrated that zwitterionic copolymers on a hydrophobic surface are capable of resisting protein adsorption from a single-protein solution to a level of <5 ng/cm^2 measured by a surface plasmon resonance (SPR) sensor when its surface density is controlled. However, these physically adsorbed zwitterionic copolymers are more suited for hydrophobic surfaces. It is desirable to develop a copolymer suitable for nonfouling coatings on charged surfaces since many biomaterials surfaces are polar/hydrophilic but not blood-inert.[3,39,40]

Previous studies show that the control of surface grafting density is important for a zwitterionic surface with superlow fouling properties.[28–30,41,42] It was reported that the chemically immobilized zwitterionic brushes provide excellent resistance to nonspecific protein adsorption from single-protein solutions and complex medium when surface grafting of a zwitterionic layer is controlled with an optimized film thickness.[42] However, at present it is still unclear how changes in the grafting coverage or packing density of zwitterionic brushes would influence platelet adhesion or cell adhesion from human blood. One current challenge is to develop reliable biomaterials, using a robust grafting strategy, with effective antithrombogenic capabilities when they are in contact with human blood.

In this work, ion-pair anchoring of ionic-zwitterionic polymer brushes onto charged biomaterial surfaces via a charge-controlled grafting-to approach is proposed. Ionic-zwitterionic copolymers with well-controlled charged block chain lengths were synthesized via atom transfer radical polymerization (ATRP), including nine zwitterionic copolymers containing anionic and zwittterionic blocks of poly(11-mercaptoundecyl sulfonic acid)-*block*-poly(sulfobetaine methacrylate) (PSA-*b*-PSBMA). These copolymers were grafted onto a positively charged surface as a mimic polar/hydrophlic biomaterial surface with controlled surface coverage or packing density so as to achieve high resistance to nonspecific protein adsorption from complex media such as whole blood. These zwitterionic anchoring surfaces were evaluated for plasma protein adsorption, blood platelet adhesion and activation, and blood cell attachment. This study not only demonstrates a grafting-to approach that achieves a stable blood-inert biomaterial surface in complex media such as human plasma and whole blood, but also provides a fundamental understanding of the correlations between polymer chain length/interfacial grafting coverage and blood compatibility. There are three unique aspects of this work: a) the demonstration of a surface resisting protein adsorption from human whole blood; b) a systematic study of the effects of the molecular weights and packing densities of grafted polymer brushes on blood compatibility; and c) the development of a convenient method to create blood-inert surfaces by grafting zwitterionic-ionic copolymers to charged biomaterials.

2. Results and Discussion

2.1. Polymerization of Ionic-Zwitterionic Block Copolymers

To study the effects of the surface coverage of the surface-anchored PSBMA brushes on blood-inert properties, nine different ionic-zwitterionic diblock copolymers, PSA-*b*-PSBMA, were synthesized in this work. A summary of average molecular weights, various block compositions, and solution characteristics of prepared copolymers is given in **Table 1**. The

Table 1. Characteristics of PSA-*b*-PSBMA copolymers.

Sample ID[a)]	Characterization of copolymers[b)]		Degree of polymerization		Zeta potential[c)]	Hydrodynamic size[c)]
	M_w [kDa]	M_w/M_n	m	n	φ [mV]	D_H [nm]
PSA_{10}-*b*-$PSBMA_{10}$	4.8	1.2	11	8	–0.1	<10
PSA_{20}-*b*-$PSBMA_{10}$	7.9	1.2	23	8	–0.7	<10
PSA_{40}-*b*-$PSBMA_{10}$	13.4	1.3	46	8	–0.9	10
PSA_{10}-*b*-$PSBMA_{20}$	10.3	1.4	13	25	–0.3	<10
PSA_{20}-*b*-$PSBMA_{20}$	11.6	1.3	19	25	–0.5	<10
PSA_{40}-*b*-$PSBMA_{20}$	17.1	1.2	41	25	–2.8	11
PSA_{10}-*b*-$PSBMA_{40}$	15.0	1.4	12	43	–0.4	10
PSA_{20}-*b*-$PSBMA_{40}$	18.1	1.2	24	43	–2.4	11
PSA_{40}-*b*-$PSBMA_{40}$	23.0	1.3	44	43	–3.7	12

[a)]The ratio of initiator/Cu(I)Br/bpy was 1:1:2; [b)]Weight-average molecular weights (M_w) and molecular weight distributions (M_w/M_n) were estimated by GPC and calibrated with PEO; [c)]Zeta potential and hydrodynamic diameter of suspended PSA-*b*-PSBMA copolymers in PBS at 37 °C were estimated by dynamic light scattering.

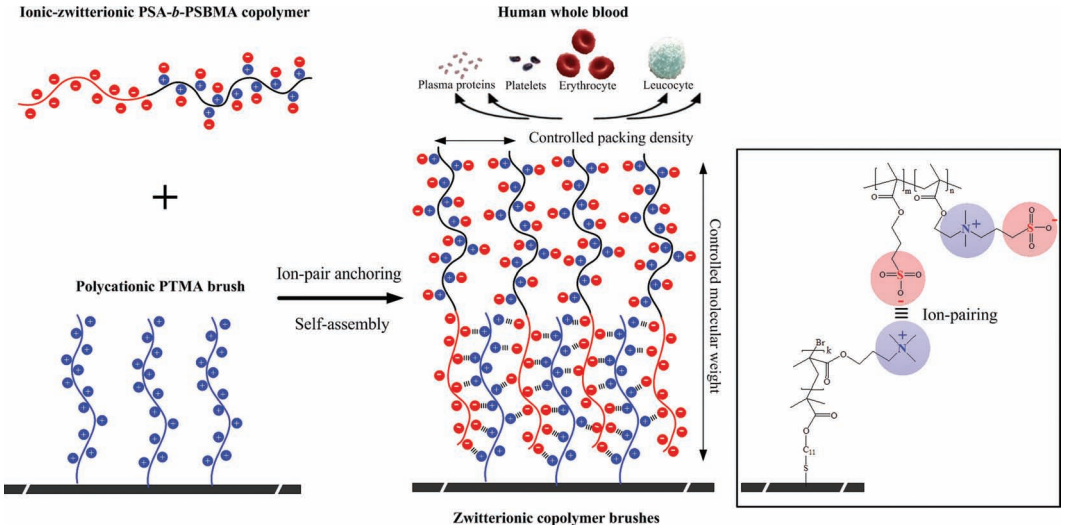

Scheme 1. Ion-pair anchoring of zwitterionic copolymer brushes.

degree of polymerization (D_p: m or n) of each block was controlled by the initial molar ratio of monomer to initiator. Low polydispersities of the initial PSBMA homopolymers of less than 1.18 were obtained, which confirms the good living characteristics of this first-stage ATRP polymerization. The final PSA-*b*-PSBMA copolymers obtained had a relatively high molecular weight (M_w), ranging from 4.8 kDa to 23.0 kDa, which indicates the retained living characteristics of this second-stage polymerization.

The zeta potential and hydrodynamic diameter of the copolymers in soluble unimer state was estimated by dynamic light scattering (DLS; Malvern Zetasizer Nano ZS) at a polymer concentration of 1 mg/mL in PBS solution. Increasing the M_w of PSA block in the prepared copolymers increased the negative zeta potential and hydrodynamic diameter of the PSA-*b*-PSBMA suspension, while the chain length of PSBMA was kept constant. This may be attributable to the increase in the polymer chain length of anionic sulfonate groups in the PSA block, contributing to an increase in the available negative charge. The polymer hydrodynamic size as the D_p of PSA block was increased in a range from 10 to 40. For the case of copolymers PSA_{40}-*b*-$PSBMA_{10}$, PSA_{40}-*b*-$PSBMA_{20}$, and PSA_{40}-*b*-$PSBMA_{40}$, interestingly, an unusual antipolyelectrolyte behavior in the presence of PBS medium was observed: The overall negative charge of prepared copolymers was notably enhanced with the increased M_w of PSBMA block in the prepared copolymers as the D_p of PSA block was controlled in a range close to 40. The dependence of the dissolution process of PSA block on the increased chain length of zwitterionic PSBMA block was attributed to the screening of the net attractive electrostatic interactions between the anionic polymer chains by salt ions. This effect led to copolymer chain expansion, resulting in the exposure of anionic sulfonate groups in the PSA block, and contributing to an increase in the overall negative charge of the prepared PSA-*b*-PSBMA copolymers. It is expected that the stronger expression of the negatively charged block in the zwitterionic copolymer would result in more stable anchoring on a positively charged surface.

2.2. Surface Anchoring with Ionic–Pair Self-Assembly of PSA-*b*-PSBMA

The physical grafting of well-defined PSA-*b*-PSBMA diblock copolymers onto the cationic PTMA brush surfaces was performed to study the blood-inert characteristics of zwitterionic sulfobetaine groups in the PSBMA block. The anionic sulfonate group in the PSA block was used as the charged moiety of the PSA-*b*-PSBMA copolymers which mediate electrostatic interaction with cationic PTMA brushes. To achieve consistent grafting qualities of surface anchoring with PSA-*b*-PSBMA copolymers, all polymer brushes of PTMA were prepared by surface-initiated ATRP with a controlled film thickness of 40 ± 5 nm as measured by ellipsometry. The molecular structure of ionic-pair self-assembly of PTMA brushes anchored with PSA-*b*-PSBMA is shown in **Scheme 1**. The ideal model of this self-assembly process is performed by in situ observation using a SPR sensor to directly provide the correlation between the zwitterionic surface coverage and packing densities from different surface-anchored PSA-*b*-PSBMA copolymers with the adsorption of single protein or plasma proteins in various controlled media.

PSA-*b*-PSBMA diblock copolymers were first physically adsorbed onto the SPR sensor surfaces, grafted by cationic PTMA brushes via the ionic-pair self-assembly of PSA-PTMA electrostatic interactions, followed by the in situ evaluation of plasma protein adsorption on the surfaces with surface-anchored PSA-*b*-PSBMA copolymers. The adsorbed amounts of both copolymers and proteins were measured and compared by SPR (**Figure 1**). For the stage of self-assembled PSA-*b*-PSBMA surface formation, the copolymer anchoring amount (Figure 1a) is defined as the SPR wavelength difference between the two baselines established before and after copolymer adsorption. It can be seen from the SPR sensorgram that the quick increase in wavelength after addition of copolymer suggests the fast polymer adsorption onto the bare PTMA brushes, which depends on the PSA-*b*-PSBMA concentration in PBS ($C_{PSA\text{-}b\text{-}PSBMA}$). After that, since the electrostatic

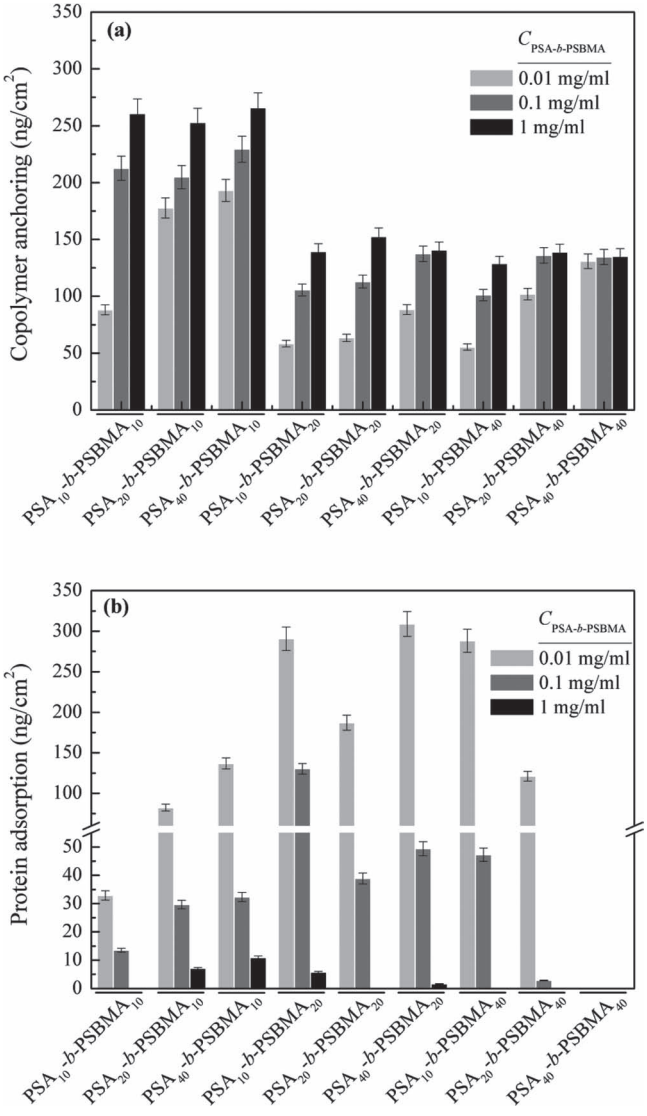

Figure 1. Amount of a) copolymer anchoring and b) protein adsorption on different PSA-*b*-PSBMA anchored surfaces with the concentration of copolymer solution ($C_{PSA-b-PSBMA}$) in 0.01, 0.1, and 1 mg/mL at 23 °C as measured by SPR.

interaction sites on the PTMA brushes were mostly occupied, the adsorbed polymers primarily underwent structural reorganization and reversible attachments on the surface, thus leading to the slow kinetics of polymer adsorption. After 35 min of polymer injection, PBS was used to flush away weakly bound polymers on the surface for 50 min, reaching a steady plateau. To study the effects of the surface coverage and packing density of physically anchored copolymers on protein resistant characteristics, nine different PSA-*b*-PSBMA diblock copolymers were used in this study. Physical characteristics of these nine PSA-*b*-PSBMA diblock copolymers are summarized in Table 1. It is expected that these well-defined diblock copolymers have different surface packing densities, which results in different protein adsorption behavior. For the subsequent stage of protein adsorption on PSA-*b*-PSBMA anchored surface, the protein adsorption amount (Figure 1b) is defined as the SPR wavelength difference between the two baselines established before and after protein adsorption.

The concentration of copolymer solution, $C_{PSA-b-PSBMA}$, was varied from 0.01 to 1 mg/mL to examine the PSA-*b*-PSBMA packing on the surface and subsequent protein adsorption. The increase of $C_{PSA-b-PSBMA}$ resulted in the increased packing density of PSA-*b*-PSBMA onto PTMA surfaces and the reduced adsorption of fibrinogen from a single protein solution. Increasing the PSA length or negative zeta potential of the PSA-*b*-PSBMA copolymers results in the decreased $C_{PSA-b-PSBMA}$ needed to achieve fully packed PSA-*b*-PSBMA grafted onto the surface. For the PSA$_{40}$-*b*-PSBMA$_{40}$ anchored surface, the saturated anchoring amount of the copolymers can be formed in a wide range of $C_{PSA-b-PSBMA}$, controlled between 0.01 and 1 mg/mL, and resulted in the zero adsorption of fibrinogen from a single protein solution. The result indicates that the perfect self-assembled packing of the PSA-*b*-PSBMA anchored surface can be controlled with the appropriate molar fraction of PSBMA to PSA ($f_{PSBMA/PSA}$) and molecular size of PSBMA or PSA blocks. For the surface anchored copolymers of PSA$_{20}$-*b*-PSBMA$_{10}$, PSA$_{40}$-*b*-PSBMA$_{10}$, and PSA$_{40}$-*b*-PSBMA$_{20}$ with the ratio of $f_{PSBMA/PSA} < 1$, fibrinogen adsorption onto the exposure charged domains of the PSA-*b*-PSBMA anchored surface is due to surface packing defects formed from the large molecular size of the negatively charged PSA block.

For the fully packed surfaces anchored copolymers of PSA$_{10}$-*b*-PSBMA$_{40}$, PSA$_{20}$-*b*-PSBMA$_{40}$, and PSA$_{40}$-*b*-PSBMA$_{40}$ with the ratio of $f_{PSBMA/PSA} \geq 1$, the zwitterionic shielding coverage of the surface-anchored PSBMA polymers is enough to resist all fibrinogen adsorption from a single protein solution while the M_w of PSBMA block was controlled in a range close to 11 kDa ($D_p \approx 43$). Importantly, it should be noted that a fibrinogen-resistant nonfouling surface can be obtained by the saturated surface anchoring of PSA$_{10}$-*b*-PSBMA$_{10}$, PSA$_{20}$-*b*-PSBMA$_{20}$, and PSA$_{40}$-*b*-PSBMA$_{40}$ with the ratio of $f_{PSBMA/PSA} \approx 1$, which is independent of the molecular size of PSA-*b*-PSBMA. Considering that blood-inert PSA-*b*-PSBMA anchored surfaces are in contact with complex media such as human serum, plasma or whole blood, it is reasonably expected that the increase of the chain length of PSA block in copolymers would enhance the electrostatic intermolecular interaction with the PTMA brushes contributed by the increased ion-pair binding sites.

Generally, a surface with a high coverage of anchored PSBMA brushes results in low protein adsorption. For the fully packed surfaces prepared from the copolymers of PSA$_{10}$-*b*-PSBMA$_{40}$, PSA$_{20}$-*b*-PSBMA$_{40}$, and PSA$_{40}$-*b*-PSBMA$_{40}$, via "graft-to" physical adsorption or from PSBMA brushes via "graft-from" ATRP, the zwitterionic coverage of the surface-anchored PSBMA polymers is high enough to resist fibrinogen adsorption from a single protein solution in PBS. The adsorption/desorption behavior of block copolymers associated with protein adsorption was tested in three different types of single protein solutions and three different types of salt solutions (Figure S1,S2 in the Supporting Information). As shown in Figure S1, the fouling resistance of PSA-*b*-PSBMA with a shorter PSA block to protein adsorption from fibrinogen, γ-globulin, and HSA in PBS buffer is reduced from cyclic protein adsorption tests,

indicating the low stability or grafting coverage of anchored PSA_{10}-*b*-$PSBMA_{40}$. The results in Figure S2 also indicate that a shorter PSA block has weaker ion-pair electrostatic interaction, leading to the lower stability of surface anchoring in aqueous solutions with three different ionic salts of NaCl, KCl, and NH_4Cl at low ionic strengths (below 0.15 M). The results clearly support that PSA-*b*-PSBMA polymers with lower molecular weights of PSA blocks have weaker electrostatic interactions at ion-pair anchoring interface, leading higher protein fouling and poorer blood compatibility.

2.3. Plasma Protein Adsorption and Blood Platelet Adhesion

It is widely believed that surface resistance to plasma protein adsorption and blood platelet adhesion is essential to achieve a blood-inert surface for human blood-contacting biomaterials. Fibrinogen in blood plasma is particularly important for platelet adhesion since it can bind to the platelet GP IIb/IIIa receptor. From Figure 1, it can be seen that all the surfaces fully anchored with PSA-*b*-PSBMA copolymers exhibit fibrinogen adsorption of <10 ng/cm^2 from single protein solution, which are considered to be ultralow fouling surfaces. For PSA_{10}-*b*-$PSBMA_{10}$, PSA_{20}-*b*-$PSBMA_{20}$, PSA_{10}-*b*-$PSBMA_{40}$, PSA_{20}-*b*-$PSBMA_{40}$, and PSA_{40}-*b*-$PSBMA_{40}$, these PSA-*b*-PSBMA fully anchored surfaces can strongly resist non-specific fibrinogen adsorption to 0 ng/cm^2. However, human blood serum and plasma pose significant challenges to blood-contacting biomaterials because of their high nonspecific protein adsorption onto general surfaces. Blood plasma is a multicomponent solution containing sugars, fats, amino acids, urea, and a very large number of proteins. It should be pointed out that there are clotting-induced proteins in blood plasma but not in blood serum. Here, the extent of nonspecific protein adsorption from human serum and plasma was evaluated by SPR measurement for the inspection of blood compatibility of the surfaces fully anchored with PSA_{20}-*b*-$PSBMA_{40}$ and PSA_{40}-*b*-$PSBMA_{40}$ copolymers, which provide excellent resistance of single-protein fibrinogen adsorption. Hydrophobic CH_3-SAMs and zwitterionic PSBMA brushes were used as references. Real-time adsorption of human serum or plasma proteins onto reference surfaces and PSA-*b*-PSBMA anchored surfaces was monitored using SPR at 37 °C. It should be noted that the response of the SPR, with broader sense of adsorption from 20–100% serum or 20–100% plasma solution, is not only to major components of plasma proteins, but also to other small biomolecules, such as lipids and polysaccharides. However, it is accepted that the major change of the SPR signal is attributed mainly to the higher molar mass of plasma proteins, rather than other small biomolecules in serum or plasma solution. Hydrophobic CH_3-SAMs have high non-specific protein adsorption, which is also observed in **Figure 2**. Protein adsorption on hydrophobic CH_3-SAMs from 20–100% human plasma is higher than that from 20–100% human serum, indicating the components of non-specific protein adsorption containing the certain amounts of clotting-induced proteins, such as fibrinogen. Results from SPR measurements show that the PSBMA surfaces were almost completely resistant to the adsorption of non-specific proteins in both 20% human serum and 20% human plasma. However, it was observed that non-specific protein adsorption of <10 ng/cm^2 on the PSBMA surfaces from 50–100% human serum and 50–100% human plasma, which exhibit as an ultra-low fouling surface. Before self-assembled anchoring of PSA-*b*-PSBMA copolymers, the adsorption of serum and plasma proteins onto positively charged PTMA surfaces is higher than that onto hydrophobic CH_3-SAMs, indicating that electrostatic interaction enhances protein adsorption from blood serum or plasma solution. It was found that the relative amount of protein adsorption onto each sample surface is increased with the protein concentration controlled from 20% to 100% of blood serum or plasma solution. In Figure 2, it can be seen that the PSA_{40}-*b*-$PSBMA_{40}$ anchored surfaces reduced the serum and plasma protein adsorption to a level comparable with adsorption on the surfaces grafted with PSBMA brushes. However, the adsorption of serum proteins onto the surface anchored with PSA_{20}-*b*-$PSBMA_{40}$ is much higher than that with PSA_{40}-*b*-$PSBMA_{40}$. With the decrease of chain length of the negatively charged PSA block, a certain amount of the copolymers might be displaced from the surface by the serum proteins. Importantly, a comparable adsorption amount of serum and plasma proteins on PSA-*b*-PSBMA anchored surfaces indicates stable resistance of clotting-induced proteins onto the surfaces

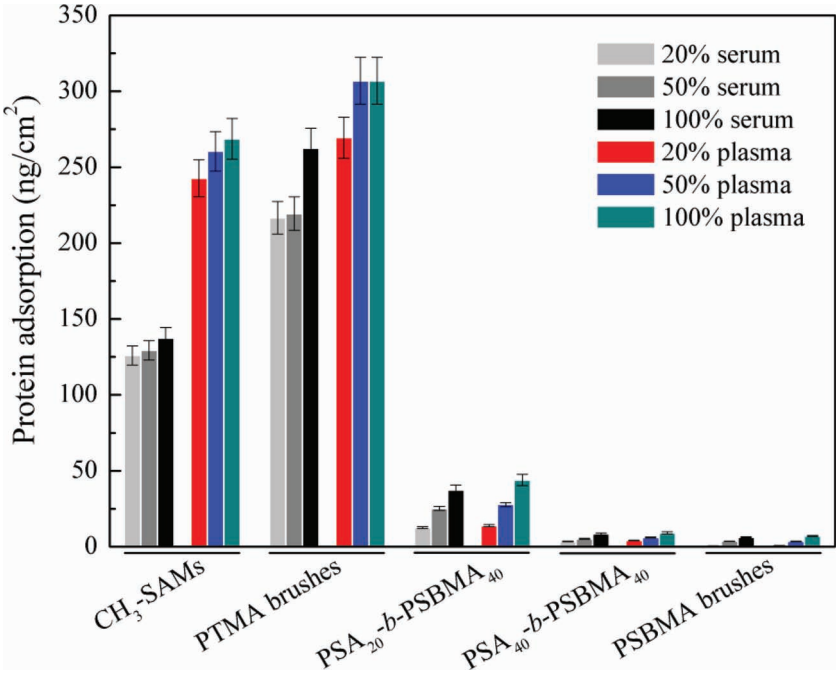

Figure 2. Adsorption of proteins onto the surfaces of CH_3-SAMs, PTMA brushes, PSA_{20}-*b*-$PSBMA_{40}$ and PSA_{40}-*b*-$PSBMA_{40}$ anchored copolymers, and PSBMA brushes from 20–100% blood serum and 20–100% blood plasma at 37 °C as measured by SPR.

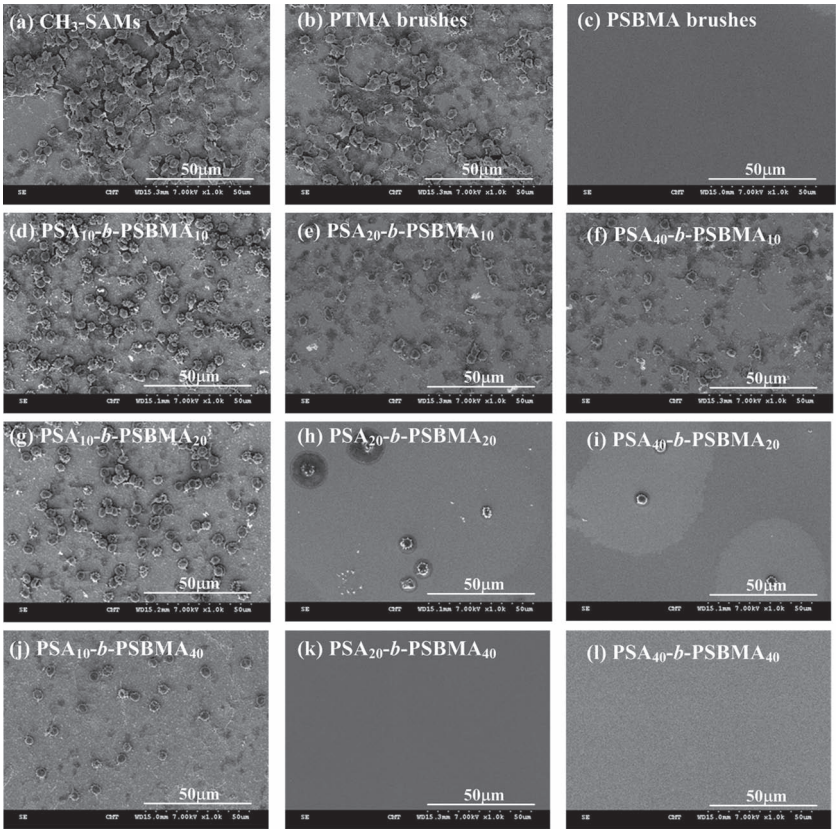

Figure 3. SEM images of human blood platelets adhered onto the surfaces of a) CH_3-SAMs, b) PTMA brushes, c) PSBMA brushes, and d–l) PSA-*b*-PSBMA anchored copolymers at 37 °C from 100% PRP. All images are at a magnification of 1000×.

from 20–100% blood plasma, which can be further estimated by the blood platelet adhesion test.

Previous studies showed that nonspecifically adsorbed plasma proteins interact in a series of reactions leading to plasma clotting.[4,5] Among plasma proteins, fibrinogen plays a leading role in mediating surface-induced adhesion and activation of platelets in human blood plasma under static conditions.[9] **Figure 3** shows SEM photographs of platelets that adhered to and activated the surfaces by contact of the prepared substrates with platelet-rich plasma solution for 60 min at 37 °C in vitro. SEM results show that no platelet attachment was observed on PSBMA brushes as compared with the hydrophobic surface (CH_3-SAMs) and positively charged surface (PTMA brushes). It is clearly observed that platelets have spread on CH_3-SAMs and PTMA brushes, which indicates the activation of adhered platelets. For the surface-anchored copolymers of PSA-*b*-PSBMA with the ratio of $f_{PSBMA/PSA} > 1$, we observed significant decreases in the adhesion and activation of platelets on copolymer anchored surfaces while the chain length of the zwitterionic PSBMA block is increased, as shown in the sequence of images in Figure 3d,g,j,k. The results indicate the importance of zwitterionic surface coverage from the controlled chain length of PSBMA block for the resistance of platelet adhesion. However, it is also important to consider the stability of anchored copolymers associated with the chain length of PSA block. As evidenced in Figure 3d–f, g–i, and j–l, it was found that the increased chain length of PSA block in copolymers strengthens ion-pair electrostatic interactions and thus forms the high packing density and strong surface anchoring of PSA-*b*-PSBMA. For the surface anchored with PSA_{40}-*b*-$PSBMA_{40}$, the result in Figure 3l indicated that high resistance of platelet adhesion was observed, which is attributed to the balanced molecular structure of PSA and PSBMA block in copolymer, resulting in both high surface coverage and packing density of zwitterionic brushes. It was also found that no platelets adhered on the surface anchored with PSA_{20}-*b*-$PSBMA_{40}$, while the surface was shown by SPR measurement to be almost completely resistant to the adsorption of clotting–induced proteins from 100% blood plasma. The results strongly support the hypothesis that surfaces which strongly resist adsorption of specific fibrinogen or clotting–induced proteins will generally resist the adhesion and activation of blood platelets.

2.4. Blood-Inert Capability of PSA-*b*-PSBMA Anchored Surfaces in Human Whole Blood

Stable blood compatibility of biomaterials used in contact with human whole blood is highly desirable for blood-inert devices. In general, a multi-step process of plasma protein adsorption, blood platelet adhesion, and blood cell attachment strongly affect the short-term and long-term thrombotic response induced by the blood-contacting materials. In this study, the extent of blood cell attachment from human whole blood was further observed by direct blood-material contact for the inspection of overall blood compatibility of the surfaces fully anchored with different PSA-*b*-PSBMA copolymers. **Figure 4** shows CLSM images of blood cells that attached to the surfaces by contact of the prepared substrates with undiluted human whole blood for 120 min at 37 °C in vitro. Attachment of blood cells on surfaces from whole blood is considered to be a challenging process, comparable to that from platelet-rich plasma solution. The CLSM results show that no blood cell attachment was observed on the surface of PSBMA brushes from whole blood as compared with that of the full-scale attached and aggregated blood cells on the hydrophobic surface (CH_3-SAMs) and positively charged surface (PTMA brushes). It clearly shows that the excellent blood-inert nature of zwitterionic sulfobetaine structure can be achieved by the surface grated with PSBMA brushes, which was also shown in Figure 3c to completely resist platelet adhesion. From the image analysis using imaging software NIS-elements Ar, statistical quantitative data of relative blood cell attachment and blood platelet adhesion on prepared surfaces is presented in **Figure 5**. Blood cell attachment from whole blood is quite similar to blood platelet adhesion from platelet-rich plasma onto the surfaces anchored with PSA-*b*-PSBMA copolymers. The increased chain length of PSBMA

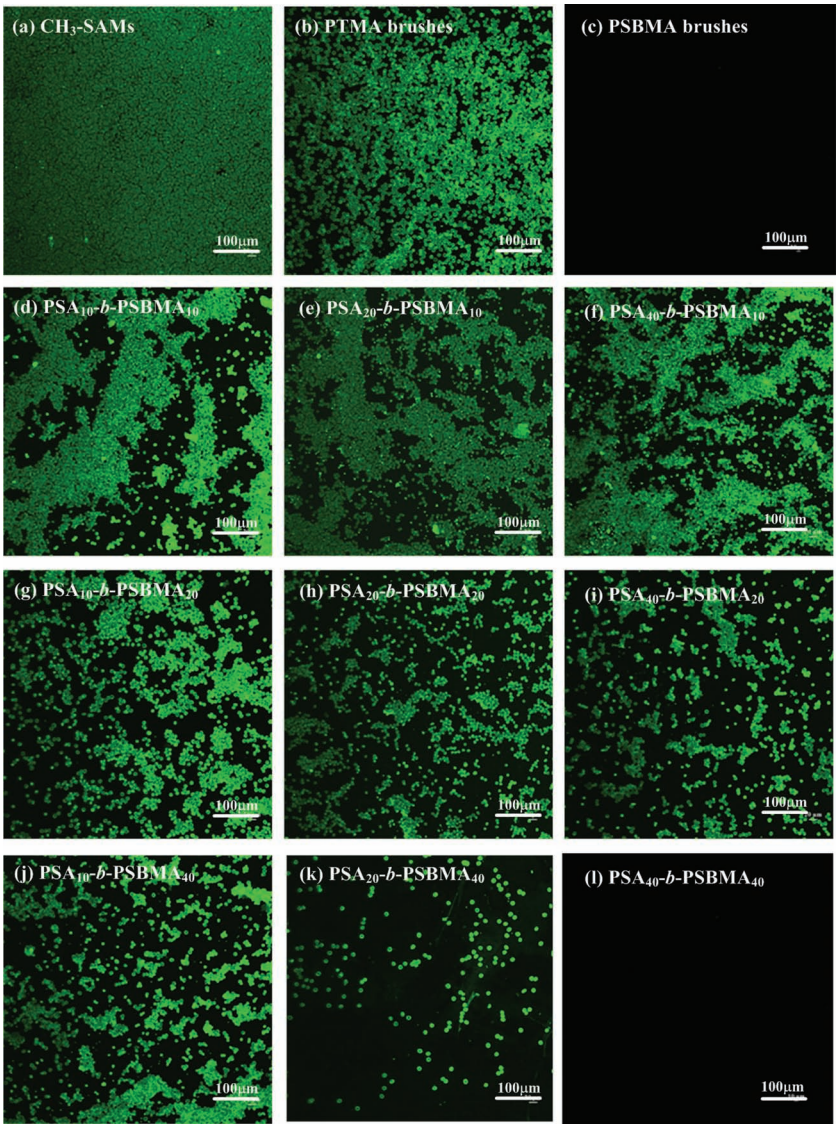

Figure 4. CLSM images of blood cells attached onto the surfaces of a) CH_3-SAMs, b) PTMA brushes, c) PSBMA brushes, and d–l) PSA-*b*-PSBMA anchored copolymers at 37 °C from human whole blood. All images are at a magnification of 1000×.

block in copolymer obviously reduced the attachment and aggregation of blood cells on surfaces, as evidenced in Figure 4d,g,j, Figure 4e,h,k, and Figure 4f,i,l. For surfaces anchored with PSA-*b*-PSBMA copolymers, shorter PSA chain length may reduce the polymer electronegativity and weaken surface ion-pair electrostatic interaction, leading to low stability of surface anchoring. However, longer PSBMA chain length may form coatings dense enough to resist protein adsorption from complex media of 100% blood serum or plasma, leading to high resistance in the following interlinked process of platelet adhesion and blood cell attachment. Importantly, the surface anchored with PSA_{40}-*b*-$PSBMA_{40}$ in Figure 3l and Figure 4l showed that the strong resistance of blood cell attachment as well as blood platelet adhesion was observed. These results indicate that ion-pair anchoring of ionic-zwitterionic copolymers, PSA-*b*-PSBMA, is able to achieve an effective nonfouling surface in human whole blood when the macromolecular size and the ratio of $f_{PSBMA/PSA}$ are properly controlled.

In this study, polycationic PTMA brushes were used as a model system to study their interaction with ionic-zwitterionic copolymers via charge pairing. The method presented in this work is applicable to many charged biomaterials. As shown in **Figure 6**, three PSA-*b*-PSBMA copolymers were grafted onto two different natural surfaces: a) chitosan films with 95% de-acetylation and b) hydroxyapatite films. Polycationic PTMA brushes grafted from a gold surface were used as reference system. Fibrinogen adsorption from 100% platelet-poor plasma onto these PSA-*b*-PSBMA anchored surfaces with different grafting coverage was measured by enzyme-linked immunosorbent assay (ELISA) with monoclonal antibodies. The quantification of protein adsorption for the PSA_{10}-*b*-$PSBMA_{40}$, PSA_{20}-*b*-$PSBMA_{40}$, and PSA_{40}-*b*-$PSBMA_{40}$ anchored surfaces with the copolymer solution concentration ($C_{PSA\text{-}b\text{-}PSBMA}$) of 0, 0.01, and 1.0 mg/mL at 23 °C was normalized by the amounts of protein adsorption in each individual virgin sample of chitosan films, hydroxyapatite films, and PTMA brushes. The relative fibrinogen adsorption was shown to be correlated with zwitterionic surface coverage and packing densities from different surface-anchored PSA-*b*-PSBMA copolymers in various controlled $C_{PSA\text{-}b\text{-}PSBMA}$. For PSA_{40}-*b*-$PSBMA_{40}$ anchored surfaces with $C_{PSA\text{-}b\text{-}PSBMA}$ in 1 mg/mL, it was found that the relative amounts of protein adsorption were all controlled less than 10% of that on the uncoated sample, indicating that anchored PSBMA brushes via charge pairing highly reduced plasma protein adsorption from 100% human plasma. It was found that chitosan and hydroxyapatite films grafted with longer PSA blocks and higher concentration of PSA_{20}-*b*-$PSBMA_{40}$ and PSA_{40}-*b*-$PSBMA_{40}$ copolymers were highly resistant to nonspecific plasma adsorption from fresh human plasma solution at 37 °C, whereas PSA_{10}-*b*-$PSBMA_{40}$ showed high protein adsorption. The results are consistent with previous findings of protein adsorption on PSA-*b*-PSBMA anchored surfaces in Figure 1b and Figure 2. The present method for preparing blood-inert surfaces via ion-pair anchoring of zwitterionic copolymer brushes can be applicable to biomaterials in real-world applications with charged surfaces.

3. Conclusions

In this work, ion anchoring of the ionic-zwitterionic block copolymers PSA-*b*-PSBMA onto charged surfaces was

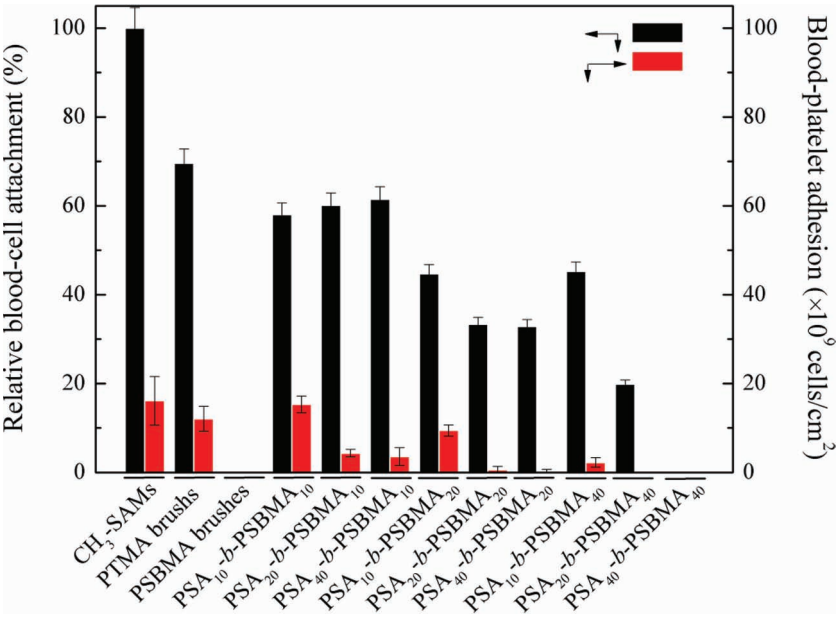

Figure 5. Quantitative analysis of the changes in blood cell attachment and blood platelet adhesion on the surfaces of CH_3-SAMs, PTMA brushes, PSBMA brushes, and PSA-*b*-PSBMA anchored copolymers at 37 °C from human whole blood and platelet-rich plasma, respectively.

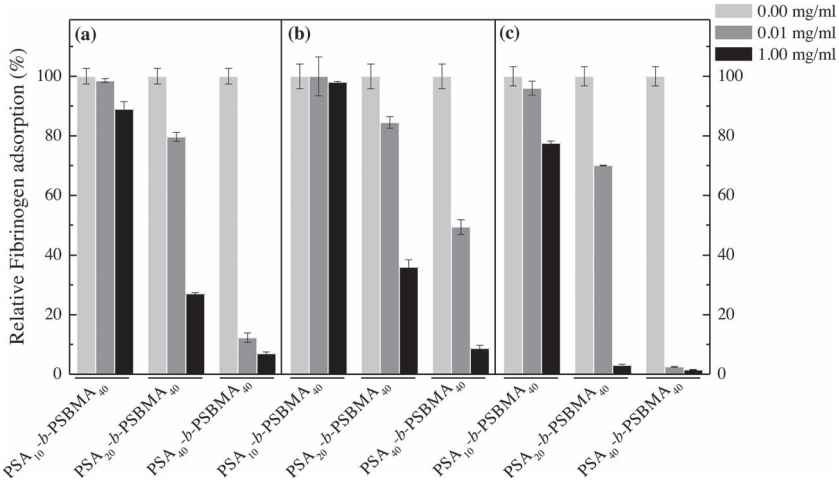

Figure 6. Relative human fibrinogen adsorption from 100% platelet-poor plasma solution on surfaces of a) chitosan film, b) hydroxyapatite film, and c) PTMA brushes grafted from a gold surface anchored with PSA_{10}-*b*-$PSBMA_{40}$, PSA_{20}-*b*-$PSBMA_{40}$, and PSA_{40}-*b*-$PSBMA_{40}$ copolymers. All data were determined from ELISA with each virgin sample as a reference, where the amount of fibrinogen adsorbed on virgin sample was normalized to unity. Data are expressed as the means ± SD of three independent measurements.

implemented via a robust graft-to approach. With well-defined diblock copolymers and well-controlled surface packing densities, surfaces covered with PSA-*b*-PSBMA brushes were shown to have excellent inert properties in complex media. Interestingly, the increase in both ionic SA and zwitterionic SBMA units in the copolymers tends to effectively reduce the adhesion and activation of platelets, even to a level of zero platelet adhesion. This work provides a platform to study how polymer molecular weights and surface packing densities will affect nonfouling properties. Under optimized conditions, PSA-*b*-PSBMA anchored surfaces with a balanced macromolecular structure of PSA block and PSBMA block can strongly resist non-specific protein adsorption (≈0 ng/cm^2 in single fibrinogen solution, and <10 ng/cm^2 in 100% human blood serum and plasma). This ion-pair anchoring strategy enables the fast, effective, and stable immobilization of PSA-*b*-PSBMA brushes directly onto charged surfaces, and provides one convenient method for surface zwitterionization. The resulting surface anchored with zwitterionic copolymer brushes maintained excellent blood-inert properties ('zero' blood platelet adhesion and blood cell attachment) when the surface is in contact with 100% platelet-rich plasma and 100% human whole blood.

4. Experimental Section

Chemicals: [2-(Methacryloyloxy)ethyl]-dimethyl-(3-sulfopropyl)-ammonium hydroxide (sulfobetaine methacrylate, SBMA) was purchased from Monomer-Polymer & Dajac Laboratories, Inc. U.S. [2-(methacryloyloxy) ethyl]trimethylammonium chloride (TMA) and 11-mercaptoundecyl sulfonic acid (SA) were purchased from Sigma Chemical Co. Chitosan HD with a degree of deacetylation of 95% was purchased from Lytone Co. Ltd. Hydroxyapatite (CAS-No.12167-74-7) containg 38.1% calcium was purchased from Sigma-Aldrich. Copper(I) bromide (99.999%), methyl 2-bromopropionate (MBrP, 98%), pyridine (98%), 2-hydroxyethyl acrylate (97%), 2,2′-bipyridine (BPY, 99%), triethylamine(99%), tetrahydrofuran (THF HPLC grade) and ethanol (absolute 200 proof) were purchased from Sigma-Aldrich. Acetic acid was from Scharlau Chemical Company INC. 1-Undecanethiol (99+%) and 11-mercapto-1-undecanol (99+%) were purchased from Asemblon INC. Fibrinogen (fraction I from human plasma), γ-globulin (Fraction II, III, 99%), human serum albumin (HSA, 96–99%) were purchased from Sigma Chemical Co. Deionized water (DI water) used in experiments was purified using a Millipore water purification system with a minimum resistivity of 18.0 MΩ· m. THF for reactions and washings were dried by sodium before use. ω-Mercaptoundecyl bromoisobutyrate was synthesized through reaction of BIBB using a method published previously.[12,31,41] ^{1}H NMR (300 MHz, $CDCl_3$): 4.15 (t, J) 6.9, 2H, OCH_2), 2.51(q, J) 7.5, 2H, SCH_2), 1.92 (s, 6H, CH_3), 1.57-1.72 (m, 4H, CH_2), and 1.24-1.40 (m, 16H, CH_2).

Preparation of PSA-b-PSBMA Diblock Copolymers: The controlled/living radical polymerization of a PSA-*b*-PSBMA diblock copolymer was carried out via the ATRP method. In this study, all of the reactions were conducted in a dry box under a nitrogen (99.99%) atmosphere. First, SBMA monomer (2.0 g, 6.77 mmol) was polymerized in 10 mL of methanol using three different molar ratios of [SBMA]/[MBrP]/[CuBr]/[bpy] = 10:1:1:2, 20:1:1:2 and 40:1:1:2, respectively, under nitrogen at 20 °C. After 24 h, the SBMA conversion was more than 99% as judged

by 1H NMR from the disappearance of vinyl signals at δ 5.5–6.0 (a Bruker 500 MHz spectrometer and D_2O as solvent), and in each case, the PSBMA homopolymer obtained had a relatively low polydispersity (i.e., M_w/M_n = 1.10-1.18). After polymerization, the resulting reaction solution was passed through an aluminum oxide column, precipitated into ethanol, and re-dissolved into water repeatedly to remove residue catalysts. After solvent evaporation, the PSBMA homopolymers were dried in a freeze-dryer at –45 °C for 24 h to yield a white powder. Then, SA monomer (2.0 g, 8.12 mmol) was polymerized with a defined molecular weight of PSBMA macroinitiator (PSBMA-Br) in 10 mL of DI water using three different molar ratios of [SA]/[PSBMA-Br]/[CuBr]/[bpy] = 10:1:1:2, 20:1:1:2 and 40:1:1:2, respectively, under nitrogen at 60 °C. After 48 h, the resulting PSA-*b*-PSBMA diblock copolymer was precipitated into THF, then re-dissolved in water, and passed through an aluminum oxide column to remove the residue catalysts. The diblock copolymer was dried by freeze-drying for 24 h to yield a white powder. In Table 1, aqueous GPC analysis indicated nine PSA-*b*-PSBMA diblock copolymers with the controlled polydispersities (i.e., M_w/M_n = 1.20–1.40). The molecular weights of the prepared PSBMA polymers and PSA-*b*-PSBMA copolymers were determined by aqueous gel-permeation chromatography (GPC), using two Viscogel columns, a G4000 PWXL and a G6000 PWXL (the range of molecular weight was from 2 kDa to 8000 kDa) connected to a model Viscotec refractive-index detector at a flow rate of 1.0 mL/min and a column temperature of 23 °C. The eluent was an aqueous solution composed of 0.1 M $NaNO_3$ at pH 7.4. Poly(ethylene oxide) (PEO) standards from Polymer Standard Service, Inc. (Warwick, USA) were used for calibration.

Preparation of Self-Assembled Monolayers on Gold Surfaces: In this work, two self-assembled monolayers (SAMs) were formed on the substrates. 1) methyl-terminated (CH_3) and 2) initiator ω-mercaptoundecyl bromoisobutyrate (Br) SAMs. BK-7 glass chips (SCHOTT Taiwan Ltd.) and P(100) Si wafers (Wafer Works Corporation Co., Inc.) were first coated with an adhesion-promoting chromium layer (thickness 2 nm) and a surface plasmon active gold layer (48 nm) by electron beam evaporation under vacuum. Before SAM preparation, the gold-coated substrate was cleaned by washing with pure ethanol and distilled water in sequence, dried with N_2, then left in an UV light cleaner for 20 min at a source power of 110 W, followed by rinsing with distilled water and ethanol, and finally dried with N_2. For preparation of CH_3-SAMs, the cleaned chip was soaked in a 2 mM ethanol solution of 1-undecanethiol thiols for 24 h to form SAMs on the gold surface, and the chip was rinsed in sequence with ethanol and water, and then dried in a stream of N_2. For the preparation of an initiator SAM on a gold surface, the cleaned chip was soaked in a 2 mM ethanol solution of ω-mercaptoundecyl bromoisobutyrate for 24 h to form Br-SAMs on the gold surface, and the chip was rinsed with pure ethanol followed by THF and then dried in a stream of N_2.

Preparation of PSBMA and PTMA Homopolymer Brushes: Two well-packed homopolymer brushes of poly(sulfobetaine methacrylate) (PSBMA) and poly(11-mercapto-*N*,*N*,*N*-trimethylammonium chloride) (PTMA) on SPR glass chips and Si wafers were achieved via the surface-initiated ATRP method, which were prepared the following method reported previously.[12,32] These homopolymer brushes were polymerized on the gold substrates with immobilized initiators of Br-SAMs based on previous reports. The reaction solution of CuBr and BPY were first placed in a sealed glass reactor in a dry box under nitrogen atmosphere. A 400 mM degassed solution (pure water and methanol in a 1:3 volume ratio) with monomers was transferred to the reactor and the gold surface with immobilized initiators was then placed in the reactor under nitrogen. After polymerization, the substrate was removed and rinsed with ethanol and water, and the samples were kept in water overnight. The prepared substrates were rinsed with PBS buffer to remove unbound polymers before any experiments. The thickness of the substrates was measured by ellipsometry. The thickness of the polymer film was controlled within a similar range of about 40 ± 5 nm. The details about polySBMA film thickness as a function of polymerization time for different SBMA concentrations was reported in previous studies.[12,32]

Preparation of Surface Anchoring Zwitterionic Copolymer Brushes: The physisorption of the prepared zwitterionic copolymers onto SPR glass chips and Si wafers grafted with ionic brushes was performed to study the blood-inert characteristics of copolymer anchored surfaces. As illustrated in Scheme 1, anionic sulfonate groups in the PSA block were used as the charged moiety of the PSA-*b*-PSBMA copolymers that mediate electrostatic interaction with cationic PTMA brushes. Then, it was followed by the in situ evaluation of plasma protein adsorption by SPR measurements and ex situ measurement of blood platelet adhesion and blood cell attachment on the surfaces with anchored zwitterionic copolymers by SEM observation. In the first stage of the copolymer coated surface formation, the amount of adsorbed copolymer is defined as the SPR wavelength difference between the two baselines established before and after copolymer adsorption. The saturated adsorbed amounts for each prepared copolymer on the surfaces can be obtained by the control of mass concentrations of PSA-*b*-PSBMA copolymer solution in a range of 0.01–1.0 mg/mL. A surface-sensitive SPR detector was used to monitor polymer–surface interactions in real time. The wavelength shift was used to measure the change in surface anchoring amount (mass per unit area) of the PSA-*b*-PSBMA copolymers. The calibration of the wavelength shift from SPR data associated with the amount of anchored copolymers was calculated.[43] The calibration coefficient is proportional to their molar weight and depends on the resonant wavelength. For the SPR sensor used in this study (resonant wavelength around 780 nm), a 1 nm SPR wavelength shift represents a change in the copolymer surface coverage of 22 ng/cm^2.[43–45]

Real-Time Protein Adsorption: In this work, a custom-built SPR biosensor based on wavelength interrogation with a four-channel Teflon flow cell was used to monitor protein adsorption on the treated substrate. A SPR sensor chip was attached to the base of the prism and optical contact was established using refractive index matching fluid (Cargille). Single protein solution of 1.0 mg/mL human fibrinogen in phosphate buffered saline (PBS, 0.15M, pH 7.4) was delivered to the surfaces at a flow rate of 0.05 mL/min. In this study, 20–100% blood serum and 20–100% blood plasma solutions containing plasma proteins in PBS were flowed through independent channels for 20 min, followed by PBS buffer solution to remove unbound protein molecules and to reestablish the baseline. Protein adsorption was quantified by measuring the change in wavelength in the buffer baselines before and after protein adsorption. The wavelength change (Δn_2, nm) was converted to an amount of adsorbed protein. The calibration follows the standard calculation for the same custom-built SPR system resulting a 1 nm wavelength shift in the SPR response equivalent to about 17 ng/cm^2 of adsorbed plasma proteins.[43,46]

Blood Platelet Adhesion and Activation: The gold-coated Si wafers with SAMs (CH_3-SAMs), polymer brushes (polyTMA, and polySBMA), and copolymer brushes (PSA-*b*-PSBMA) of 1 cm^2 surface area were placed in individual wells of a 24-well tissue culture plate and each well was equilibrated with 1000 µL of PBS for 2 hr at 37 °C. Platelet rich plasma (PRP) containing about 1×10^5 blood cells/mL was prepared by centrifugation of the blood at 20 Hz (1200 rpm) for 10 min. The platelet concentration was determined by a microscopy (NIKON TS 100F). 200 µL of the PRP recalcified by addition of calcium (1 M $CaCl_2$, 5 µL) was placed on the substrate surface in each well of the tissue culture plate and incubated for 120 min at 37 °C. After the wafers were rinsed twice with 1000 mL of PBS, they were immersed into 2.5% glutaraldehyde in PBS for 48 h at 4 °C to fix the activated platelets and other adhered blood cells, then rinsed three times with 1000 mL of PBS and gradient-dried with ethanol in 75% v/v PBS, 50% v/v PBS, 25% v/v PBS, 5% v/v PBS, and 0% v/v PBS for 20 min in each step and dried in air. Finally, the samples were sputter-coated (Toshiba E-1010 ion sputter) with gold prior to observation under JEOL JSM-5410 SEM operating at 7 keV. The number of adhering platelets on the hydrogels was counted from scanning electron microscopy (SEM) images at a 5000× magnification from five different places on the same substrate. The process was repeated using three independent samples (n = 15 in total).

Whole Blood Cell Attachment: The gold-coated glass chips with SAMs (CH_3-SAMs), polymer brushes (polyTMA, and polySBMA),

and copolymer brushes (PSA-*b*-PSBMA) of 1 cm^2 surface area were placed in individual wells of a 24-well tissue culture plate and each well was equilibrated with 1000 µL of PBS for 24 h at 37 °C. 250 mL fresh whole blood obtained from five healthy human volunteers was mixed with 35 mL citrate phosphate dextrose adenine-1 (CPDA-1). 1000 µL of whole blood was placed on the substrate surface in each well of the tissue culture plate and incubated for 2 h at 37 °C. After the chips were rinsed twice with 1000 mL of PBS, they were immersed in 300 µL of 4.0% formaldehyde in PBS for 15 min at 4 °C to fix the adhered blood cells, then rinsed three times with 1000 µL of PBS. Blood cells attached to the sample surfaces were stained with 3 µL of CD3-FITC, CD14-FTIC, and CD45-FITC in 270 µL of PBS with 2.5% glutaraldehyde at 4 °C for 15 min. After washing with PBS three times, the morphology of adhered blood cells on the substrates in PBS was observed from confocal laser scanning microscopy (CLSM) images at a 200× magnification from five different places on the same chip. During observation, the images were taken at λ_{ex} = 488 nm/λ_{em} = 520 nm for detection of the FITC dye. This analysis was performed using a NIKON CLSM A1R instrument.

Plasma Protein Adsorption: In this study, platelet-poor plasma solution containing plasma proteins was tested on two biomaterial surfaces (i.e., chitosan and hydroxyapatite films) and the reference surface (i.e., PTMA brushes) anchored with the copolymers of PSA_{10}-*b*-$PSBMA_{40}$, PSA_{20}-*b*-$PSBMA_{40}$, and PSA_{40}-*b*-$PSBMA_{40}$. Blood was obtained from a healthy human volunteer. Platelet-poor plasma was prepared by centrifugation of the blood at 3000 rpm for 10 min. The fibrinogen adsorption of human plasma solution on the sample surfaces was evaluated, respectively, using the enzyme-linked immunosorbent assay (ELISA) according to the standard protocol as described briefly below. First, the samples of 1.13 cm^2 surface area were placed in individual wells of a 24-well tissue culture plate and each well was equilibrated with 1000 µL of PBS for 60 min at 37 °C. Then, the samples were soaked in 500 µL of 100% platelet-poor plasma solution. After 180 min of incubation at 37 °C, the samples were rinsed five times with 500 µL of PBS and then incubated in bovine serum albumin (BSA, purchased from Aldrich) for 90 min at 37 °C to block the areas unoccupied by protein. The samples were rinsed with PBS five times more, transferred to a new plate, and incubated in a 500 µL PBS solution. The membranes were incubated with primary monoclonal antibody that reacted with the human fibrinogen protein for 90 min at 37 °C and then blocked with 10 mg/mL BSA in PBS solution for 24 h at 37 °C. The samples were subsequently incubated with the secondary monoclonal antibody, horseradish peroxidase (HRP)-conjugated immunoglobulins for 60 min at 37 °C. The samples were rinsed five times with 500 µL of PBS and transferred into clean wells, followed by the addition of 500 µL of PBS containing 1 mg/mL chromogen of 3,3′,5,5′-tetramethylbenzidine, 0.05 wt% Tween 20, and 0.03 wt% hydrogen peroxide. After incubation for 20 min at 37 °C, the enzyme-induced color reaction was stopped by adding 500 µL of 1 mmol/mL H_2SO_4 to the solution in each well and finally the absorbance of light at 450 nm was determined by a microplate reader. Protein adsorption on the samples was normalized with respect to that on their virgin samples as a reference. These measurements were carried out 3 times for each membrane (n = 3).

Supporting Information

Supporting Information is available from the Wiley Online Library or from the author.

Acknowledgements

The authors would like to acknowledge the Center-of-Excellence (COE) Program on Membrane Technology from the Ministry of Education (MOE), R.O.C., and the National Science Council (NSC 99-2628-E-033-001 and NSC 100-2628-E-033-001-MY3) for their financial support. This work was also supported by the Office of Naval Research (N000140910137).

Received: May 22, 2012
Revised: August 17, 2012
Published online: September 28, 2012

[1] B. D. Ratner, *J. Biomater. Sci. Polym. Ed.* **2000**, *11*, 1107.
[2] D. G. Castner, B. D. Ratner, *Surf. Sci.* **2002**, *500*, 28.
[3] B. D. Ratner, A. S. Hoffman, F. J. Schoen, J. E. Lemons, *Biomaterials science, an introduction to materials in medicine*, Elsevier, Amsterdam, Netherlands **2004**.
[4] T. A. Horbett, *Cardiovasc. Pathol.* **1993**, *2*, 137S.
[5] J. L. Brash, T. A. Horbett, *ACS Symp. Ser.* **1995**, *602*, 1.
[6] P. Olsson, J. Sanchez, T. E. Mollnes, J. Riesenfeld, *J. Biomater. Sci. Polym. Ed.* **2000**, *11*, 1261.
[7] D. K. Han, N. Y. Lee, K. D. Park, Y. H. Kim, H. I. Cho, B. G. Min, *Biomaterials* **1995**, *16*, 467.
[8] H. Tuerk, R. Haag, S. Alban, *Bioconjugate Chem.* **2004**, *15*, 162.
[9] W. B. Tsai, *J. Biomed. Mater. Res.* **1999**, *44*, 130.
[10] E. Ostuni, R. G. Chapman, R. E. Holmlin, S. Takayama, G. M. Whitesides, *Langmuir* **2001**, *17*, 5605.
[11] Z. Zhang, M. Zhang, S. Chen, T. A. Horbett, B. D. Ratner, S. Jiang, *Biomaterials* **2008**, *29*, 4285.
[12] Y. Chang, S. H. Shu, Y. J. Shih, C. W. Chu, R. C. Ruaan, W. Y. Chen, *Langmuir* **2010**, *26*, 3522.
[13] R. S. Kane, P. Deschatelets, G. M. Whitesides, *Langmuir* **2003**, *19*, 2388.
[14] S. Chen, F. Yu, Q. Yu, Y. He, *Langmuir* **2006**, *22*, 8186.
[15] Y. He, Y. Chang, J. C. Hower, J. Zheng, S. Chen, S. Jiang, *Phys. Chem. Chem. Phys.* **2008**, *10*, 5539.
[16] *Poly(ethylene glycol) chemistry: Biotechnical and Biomedical Applications*, (Ed: J. M. Harris), Plenum Press, New York **1992**.
[17] Y. Chang, C. Y. Ko, Y. J. Shih, D. Quemener, A. Deratani, T. C. Wei, D. M. Wang, J. Y. Lai, *J. Membr. Sci.* **2009**, *345*, 160.
[18] Y. Chang, Y. J. Shih, C. Y. Ko, J. F. Jhong, Y. L. Liu, T. C. Wei, *Langmuir* **2011**, *27*, 5445.
[19] P. Harder, M. Grunze, R. Dahint, G. M. Whitesides, P. E. Laibinis, *J. Phys. Chem. B* **1998**, *102*, 426.
[20] W. Feng, J. Brash, S. P. Zhu, *J. Polym. Sci. Part A Polym. Chem.* **2004**, *42*, 2931.
[21] D. Leckband, S. Sheth, A. Halperin, *J. Biomater. Sci. Polym. Ed.* **1999**, *10*, 1125.
[22] Y. Iwasaki, K. Ishihara, *Anal. Bioanal. Chem.* **2005**, *381*, 534.
[23] S. Chen, S. Jiang, *Adv. Mater.* **2008**, *20*, 335.
[24] S. Jiang, Z. Q. Cao, *Adv Mater.* **2010**, *22*, 920.
[25] K. Ishihara, H. Oshida, Y. Endo, T. Ueda, A. Watanabe, N. Nakabayashi, *J. Biomed. Mater. Res.* **1992**, *26*, 1543.
[26] M. Kojima, K. Ishihara, A. Watanabe, N. Nakabayashi, *Biomaterials* **1991**, *12*, 121.
[27] N. Nakabayashi, D. F. Williams, *Biomaterials* **2003**, *24*, 2431.
[28] W. Feng, J. L. Brash, S. Zhu, *Biomaterials* **2006**, *27*, 847.
[29] Y. Chang, S. Chen, Z. Zhang, S. Jiang, *Langmuir* **2006**, *22*, 2222.
[30] J. Ladd, Z. Zhang, S. Chen, J. C. Hower, S. Jiang, *Biomacromolecules* **2008**, *9*, 1357.
[31] S. F. Chen, J. Zheng, L. Y. Li, S. Y. Jiang, *J. Am. Chem. Soc.* **2005**, *127*, 14473.
[32] Y. Chang, S. C. Liao, A. Higuchi, R. C. Ruaan, C. W. Chu, W. Y. Chen, *Langmuir* **2008**, *24*, 5453.
[33] W. Yang, S. Chen, H. Cheng, H. Vaisocherova, *Langmuir* **2008**, *24*, 9211.
[34] Y. J. Shih, Y. Chang, *Langmuir* **2010**, *26*, 17286.

[35] Y. Chang, S. Chen, Q. Yu, Z. Zhang, M. Bernards, S. Jiang, *Biomacromolecules* **2007**, *8*, 122.
[36] A. T. Nguyen, J. Baggerman, J. M. J. Paulusse, C. J. M. van Rijn, H. Zuilhof, *Langmuir* **2011**, *27*, 2587.
[37] Y. Chang, W. J. Chang, Y. J. Shih, T. C. Wei, G. H. Hsiue, *ACS Appl. Mater. Interfaces* **2011**, *3*, 1228.
[38] Y. Chang, Y. Chang, A. Higuchi, Y. J. Shih, P. T. Li, W. Y. Chen, E. M. Tsai, G. H. Hsiue, *Langmuir* **2012**, *28*, 4309.
[39] W. M. de Vos, G. Meijer, A. de Keizer, M. A. Cohen Stuart, J. M. Kleijn, *Soft Matter* **2010**, *6*, 2499.
[40] W. H. Kuo, M. J. Wang, H. W. Chien, T. C. Wei, C. Lee, W. B. Tsai, *Biomacromolecules* **2011**, *12*, 4348.
[41] G. Li, G. Cheng, H. Xue, S. Chen, F. Zhang, S. Jiang, *Biomaterials* **2008**, *29*, 4592.
[42] W. Yang, S. Chen, G. Cheng, H. Vaisocherova, H. Xue, W. Li, J. Zhang, S. Jiang, *Langmuir* **2008**, *24*, 9211.
[43] *Surface Plasmon resonance based sensors*, Vol. *4*, (Ed: J. Homola), Springer, Berlin, Germany **2006**, p. 251.
[44] J. Homola, *Chem. Rev.* **2008**, *108*, 462.
[45] Y. Chang, W. L. Chu, W. Y. Chen, J. Zheng, L. Liu, R. C. Ruaan, A. Higuchi, *J. Biomed. Mater. Res.* **2010**, *93A*, 400.
[46] H. Vaisocherova, W. Yang, Z. Zhang, Z. Cao, G. Cheng, M. Piliarik, J. Homola, S. Jiang, *Anal. Chem.* **2008**, *80*, 7894.